Journal of Alloys and Compounds 495 (2010) 209–216

Contents lists available at ScienceDirect

Journal of Alloys and Compounds

journal homepage: www.elsevier.com/locate/jallcom

Magnetocaloric effect in rare earth-based bulk metallic glasses

Q. Luo, W.H. Wang*

Institute of Physics, Chinese Academy of Sciences, Beijing 100080, PR China

ARTICLE INFO

Article history:
Received 18 December 2009
Received in revised form 22 January 2010
Accepted 22 January 2010
Available online 2 February 2010

PACS:
81.05.Kf, 61.43.Dq, 75.50.Kj

Keywords:
Metallic glasses
Magnetocaloric effect

ABSTRACT

Magnetocaloric effect (MCE) of rare earth-based bulk metallic glasses (BMGs) and the influences of applied field, structural change induced by microalloying, aging and crystallization on the MCE are systematically investigated. For all the as-cast alloys the magnetic entropy changes ($-\Delta S_m$) compare favorably with that of pure Gd metal, some are even better. Our results indicate that the BMGs and corresponding composites induced by partial crystallization be attractive candidate for magnetic refrigerants in Ericsson-cycle. Aging and partially crystallization of Gd-based BMGs lead to the reduction of both the transition temperature and the peak value of the magnetic entropy change. However, unusual table-like shapes of the MCE are observed for the crystallized samples over wide temperature range. Although the short-range structural change due to long time aging has observable effect on MCE, the structural change induced by microalloying has less influence on MCE compared with that of some crystalline materials. The possible reasons for the good MCE in these BMGs are discussed. It is found that the field dependence of magnetic entropy change follows a power law but the exponents near the transition temperature deviate from the mean field picture, and the random magnetic anisotropy has obvious effect on the field dependence of the magnetic entropy change.

1. Introduction

Recently, the search for potential magnetic refrigerants has resulted in an extensively research in the field of magnetocaloric effect (MCE) for scientific, technological and ecological reasons [1–6]. Compared with conventional gas refrigerants, magnetic refrigerants have outstanding advantages of being much more compact, high efficiency, environmentally friendliness and working easily under a variety of environments from room temperature to cryogenic temperatures. For example, the heat-transfer medium of magnetic refrigeration, depending on the working temperature, may be water or air, and for very low temperatures, helium. It has been shown that the cooling efficiency working with gadolinium can reach 60% of the theoretical limit much better than the only about 40% in the best gas-compression refrigerators [4,5]. Magnetic refrigeration is based on the magnetocaloric effect, which is an intrinsic property of the magnetic materials and implemented by employing repeated magnetization and demagnetization under adiabatic or isothermal conditions to cool from the ambient temperature to lower temperatures. Measurement of magnetic entropy change can be used as an effective way of rapidly screening prospective magnetic refrigerant materials. Nowadays, searching for materials exhibiting large MCE as refrigerants in magnetic refrigeration in different ranges of temperatures, from close to absolute zero to well above room temperature, has been one of the important tasks of the applied physics. To obtain large MCE, the magnetic materials usually must have large enough spontaneous magnetization and a strong temperature dependence of magnetization around its phase transition temperature. Intensive works have been performed on various materials, most of which are crystalline materials possessing either first order transition or second order transition such as Gd–Si–Ge, Pr–Co–Si, Mn–Fe–P–As, La–Fe–Si and Ni–Mn(Fe)–Ga [1–8] series. It has been suggested that glassy materials are also attractive for application for magnetic refrigerants [9–17], because the metallic glassy materials display many unique properties associated with their intrinsic nature and structure, such as the tailorable features of the ordering temperature, the higher electrical resistivity and thus smaller eddy current heating, and high corrosion resistance. Accordingly, the characteristics of MCE of glassy materials have attracted increasing interest, while most of these glassy materials previously studied are in ribbon form (thickness <40 μm) [10–15,17] prepared by rapid solidification of melts at a high cooling rate of the order of 10^5–10^6 K/s.

In the last two decades, bulk metallic glasses (BMGs) obtained readily at cooling rates as low as 1–100 K/s acquired considerable interest both in scientific and technological aspects [18–29]. The BMGs possess a number of attractive properties for structural and functional applications, and in many cases these properties can be enhanced by suitable heat treatment. Very recently, a series of

* Corresponding author. Tel.: +86 10 82649198; fax: +86 10 82640223.
E-mail address: whw@aphy.iphy.ac.cn (W.H. Wang).

0925-8388/$ – see front matter © 2010 Elsevier B.V. All rights reserved.
doi:10.1016/j.jallcom.2010.01.125

Table 1
Magnetic entropy changes and related parameters upon H for various materials. The a, c and $a+c$ stand for the amorphous, crystalline and crystalline phases embedded in the amorphous matrix, respectively. The RC values are calculated by the same method.

Material	Structure	Applied field (T)	Peak of ΔS_m (J kg^{-1} K^{-1})	Transition temperature (K)	Refrigerant capacity (J kg^{-1})	Reference
$Gd_{53}Al_{24}Co_{20}Zr_3$	a	5	9.4	93	590	This work
$Gd_{33}Er_{22}Al_{25}Co_{20}$	a	5	9.47	52	574	This work
$Gd_{51}Al_{24}Co_{20}Nb_1Cr_4$	a	5	9.48	100	611	This work
$Gd_{51}Al_{24}Co_{20}Nb_1B_4$	a + c	5	7.98	74–90	504	This work
$Gd_{48}Al_{25}Co_{20}Zr_3Er_4$	a	5	9.41	84	647	This work
$Gd_{51}Al_{24}Co_{20}Zr_4Nb_1$	a	5	9.23	91	651	This work
$Gd_{51}Al_{24}Co_{20}Ce_5$	a	5	8.85	81	679	This work
$Gd_{30}Al_{25}Co_{20}Y_{20}Zr_5$	a	5	7.64	37	413	This work
$Ho_{30}Y_{26}Al_{24}Co_{20}$	a	5	10.76	5.5	241	This work
$Dy_{50}Gd_7Al_{23}Co_{20}$	a	5	9.77	26	290	This work
$Er_{50}Al_{24}Co_{20}Y_6$	a	5	15.91	8	423	This work
$(Er_{0.7}Ho_{0.2}Dy_{0.1})_{55}Ni_{25}Al_{20}$	a	5	14.02	3	277	This work
$Tb_{36}Y_{20}Al_{24}Co_{20}$	a + c	5	5.60	30	–	This work
Gd	c	5	9.8	293	–	[5]
$Gd_5Si_2Ge_{1.9}Fe_{0.1}$	c	5	7	276	360	[3]
$La_{0.8}Ca_{0.2}MnO_3$	c	1.5	5.5	230	66	[2]
$Ni_2Mn_{0.75}Cu_{0.25}Ga$	c	5	65	308	72	[28]
$MnFeP_{0.45}As_{0.55}$	c	5	18.3	306	390	[4]
$Fe_{60}Cr_{14}Cu_1Nb_3Si_{13}B_9$	a	3	0.9	226	38	[11]

heavy rare earth elements (Ho, Gd, Tb, Dy, and Er) based BMGs have been developed [24–40]. In addition to their higher electrical resistivity and tailorable nature which are also shared by glass ribbons, these bulk form glassy alloys possess especially low fabrication cost, outstanding mechanical properties and high thermally stability associated with a large supercooled temperature region resulting from their excellent glass-forming ability. In particular, the heavy rare earth-based BMGs have large magnetic moments and profuse magnetic structure. All above characters are beneficial to magnetic refrigerants. Our previous work [16] has shown that the Gd-based BMGs may be considered as suitable candidates for magnetic refrigerants. Furthermore, these BMGs possess the advantages of wide choice of alloy compositions available and much wide temperature range of the large MCE. This leads to increased refrigerant capacity and makes the BMGs attractive candidate for refrigerants in multistage magnetic refrigerators. To extend the understanding of the magnetic transition property and its relationship with MCE, and how these properties change with their atomic structure, it is necessary to study the effects of aging, crystallization and alloying on the MCE in this kind of materials.

In this paper, the MCE properties of families of heavy rare earth-based BMGs are investigated in details. The influences of applied field, and the structural change induced by microalloying or substitution, and by annealing below and above the glass transition temperature on the MCE have been carried out. Large magnetic entropy changes comparable with that of the pure Gd metal have been obtained over wide temperature range. Their broader peaks are benefited from the disordered atomic structure. Aging and partially crystallization lead to the reduction of both the transition temperature and the peak value of magnetic entropy change $-\Delta S_m$. This is due to larger clusters or other phases formed during annealing. Unusual table-like shapes of the MCE have been observed for two crystallized Gd-based samples. Compared with layered composites, the composites gained by crystallization of the BMGs take the advantage of simple manufacture. Furthermore, for the rare earth-based BMGs, the transition temperature can be finely tuned in a wide temperature range by alloying or substitution, meanwhile the excellent refrigerant capacity retains. To get further insight into the nature of MCE in the BMGs, the field dependence of magnetic entropy change has been investigated and a power law in form of $|\Delta S_m| \propto H^n$ is exhibited for $Gd_{51}Al_{24}Co_{20}Zr_4Nb_1$ and $Dy_{50}Gd_7Al_{23}Co_{20}$ BMGs. The similarities and differences in the nature of MCE of the two alloys are discussed.

2. Experimental

All the BMGs with nominal compositions listed Table 1 and in this paper were prepared by arc melting pure elements in a Ti-gettered argon atmosphere. The ingot was remelted several times and then suck-cast into a Cu mold to get a cylindrical rod 2–5 mm in diameter. Their amorphous nature was ascertained by XRD using a MAC Mo3 XHF diffractometer with Cu-Kα radiation. Thermal analysis was carried out in a Perkin-Elmer DSC-7 differential scanning calorimeter (DSC) under a purified argon atmosphere at the heating rate of 20 K/min. Calorimeter was calibrated for temperature and energy at the heating rate with high purity indium and zinc. The values of the glass transition temperature T_g, and the onset temperature for crystallization T_x were determined from the DSC traces with the accuracy of ±1 K. The isothermal annealing was performed in a furnace under a vacuum of $\sim 1.0 \times 10^{-3}$ Pa at various temperatures.

Acoustic velocities were measured in a pulse echo overlap method by a MATEC 6600 model ultrasonic system with a measure sensitivity of 0.5 ns and a carrying frequency of 10 MHz. The density was measured using the Archimedean technique and the accuracy is within 0.1%. The Young's modulus E, shear modulus G, bulk modulus K and Poisson's ratio σ were derived from the density and acoustic velocities. The temperature dependence of magnetization, isothermal magnetization and the electric resistance were measured in Physical Properties Measurement System, PPMS 6000 of Quantum Design Company.

3. Results and discussion

3.1. Formation, structural, thermal, mechanical and electric properties of BMGs

Fig. 1 shows the typical XRD patterns (measured at room temperature) of the as-cast Ho-, Dy-, Gd-based BMGs. The broad X-ray diffraction maximum and no appreciable peaks corresponding to crystalline phase indicate that full amorphous rod is obtained for all these as-cast BMGs at least 3 mm in diameter. Their amorphous nature was also ascertained by DSC. As seen in Fig. 2, the remarkable feature of the DSC trace of as-cast $Gd_{51}Al_{24}Co_{20}Zr_4Nb_1$ is an endothermic reaction due to glass transition at 598 K, and three exothermic peaks due to crystallization. The onsets of first and second crystalline temperatures T_{x1} and T_{x2} are 653 K and 639 K, respectively. Similarly, for the as-cast $Gd_{53}Al_{24}Co_{20}Zr_3$ the T_g, T_{x1} and T_{x2} are determined to be 599 K, 3658 K and 637 K, respectively. Large supercooled temperature region of nearly 50 K has been observed for the Gd-based BMGs further confirming their good glass-forming ability and high thermal stability [18–22]. The supercooled liquid in wide temperature window makes the heat treatment possible and convenient for improving the property of these alloys by annealing in this temperature region.

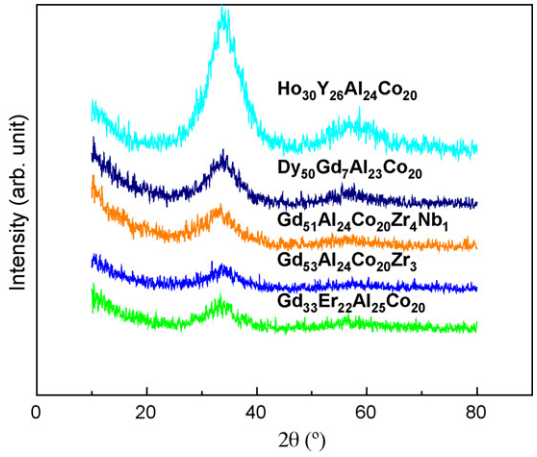

Fig. 1. XRD patterns taken from the cross-sectional slices of the as-quenched BMGs rods (diameter is 3 or 5 mm).

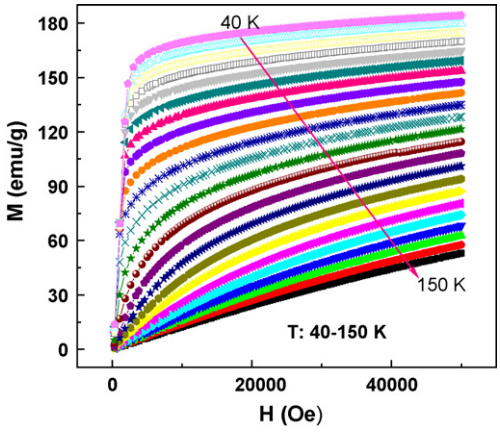

Fig. 3. Isothermal magnetization as a function of magnetic field at various temperatures for $Gd_{51}Al_{24}Co_{20}Zr_4Nb_1$.

The values of density ρ, longitudinal acoustic velocity V_l, shear acoustic velocity V_s of the as-prepared $Gd_{51}Al_{24}Co_{20}Zr_4Nb_1$ BMG are 7.314 g/cm^3, 3.529 km/s and 1.783 km/s, respectively. The E, G, K and σ thus are determined to be 61.78 GPa, 23.25 GPa, 60.09 GPa and 0.329, respectively [34–40]. The large elastic moduli, suggest the strong chemical interaction among the components and robust resistance to local structural change under crystallization, which further confirms the high thermal stability and excellent mechanical properties in this kind of materials compared with their glass ribbons. The BMGs exhibit large resistivity and negative temperature coefficient of resistivity over the whole temperature range associated with the amorphous structure [41,42]. The large electrical resistivity results in smaller eddy current heating compared with corresponding crystalline materials. Above features of the Gd-based BMGs which are beneficial for application in magnetic refrigeration are common for other heavy rare earth-based BMGs [16].

3.2. MCE properties of Gd-, Tb-, Dy-, Ho-, Er-based BMGs

The phase transition temperatures (T_c), determined at the temperature where the dM/dT displays the minimum, are 79 K and 91 K for the as-cast $Gd_{55}Ni_{25}Al_{20}$ and $Gd_{51}Al_{24}Co_{20}Zr_4Nb_1$, respectively [41]. For the as-cast amorphous alloy the magnetization varies sharply at the ordering temperature even though the strong disorder effect exists in the sample suggesting the homogeneous structure and large $|dM/dT|$ at the Curie temperature. According to the Maxwell relations, the large magnetic entropy change can be expected. A typical set of isothermal magnetization curves of M–H with increasing filed in a wide temperature range is displayed in Fig. 3 for the $Gd_{51}Al_{24}Co_{20}Zr_4Nb_1$. The sweeping rate of field is slow enough to ensure the data to be recorded in an isothermal process. Thus, the total magnetic entropy change, ΔS_m, of the system due to the application of a magnetic field can be derived from Maxwell relations by integrating over the magnetic field:

$$\Delta S_m = \int_{H_{\min}}^{H_{\max}} \left(\frac{\partial M}{\partial T}\right) dH \quad (1)$$

where $H_{\min}$ and $H_{\max}$ represent the initial and final values of magnetic field, usually $H_{\min}$ is fixed to zero. In our experiments maximal value of 5 T of the magnetic field was used.

The magnetocaloric properties of the samples are studied by evaluating the $-\Delta S_m$ from the magnetization data according to Eq. (1). The $-\Delta S_m$ as a function of temperature under field change of 2 and 5 T for these BMGs [41]. For all the samples, the positions of maximum of $-\Delta S_m$ locate in the vicinity of transition temperature in consistent with Eq. (1). For example, the peak values of $-\Delta S_m$ are 9.40 J kg^{-1} K^{-1} at 93 K, and 9.23 J kg^{-1} K^{-1} at 92.5 K for $Gd_{53}Al_{24}Co_{20}Zr_3$ and $Gd_{51}Al_{24}Co_{20}Zr_4Nb_1$, respectively. The peak and width of $-\Delta S_m$ increase obviously with increasing filed. These values of $-\Delta S_m$ are comparable with that of Gd and slightly larger than that of $Gd_5Si_2Ge_{1.9}Fe_{0.1}$ both of which are considered as good magnetic refrigerants [3]. These values are also much larger than those of most Fe- and Co-based glassy ribbons [10–15]. Fig. 4 shows that the magnetic hysteresis of the $Gd_{51}Al_{24}Co_{20}Zr_4Nb_1$ is relatively small between increasing and decreasing field even at 2 K, which is considered to be a very favorable characteristic of magnetic refrigerant application. The free of hysteresis character is expected because Gd has no orbit momentum unlike other rare earth metals, which makes the magnetocrystalline anisotropy relatively small. Therefore, it is relatively easy to magnetize and demagnetize the material without irreversible entropy production.

The remarkable feature of the shapes of $-\Delta S_m$ for the BMGs is that the large value of $-\Delta S_m$ covers a much broader temperature range compared with that of the crystalline materials. For example, in $Gd_5Si_2Ge_2$ and $MnFeP_{0.45}As_{0.55}$ (Ref. [4]) with large MCE, the temperature range of the half-maximum of the entropy change peak is less than 30 K, and in $Ni_2Mn_{1-x}Cu_xGa$ (Ref. [43]) even less than 5 K. While in $Gd_{53}Al_{24}Co_{20}Zr_3$ and $Gd_{51}Al_{24}Co_{20}Zr_4Nb_1$ BMGs the temperature ranges extend to 83 K and 75 K, respectively. This directly results in an increased refrigerant capacity (RC),

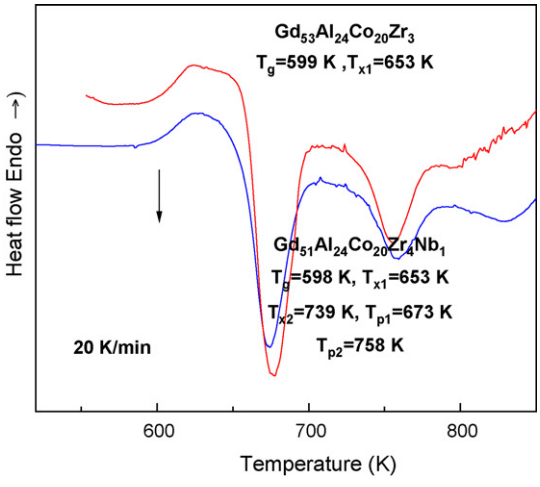

Fig. 2. DSC traces (heating rate is 20 K/min) of $Gd_{53}Al_{24}Co_{20}Zr_3$ and $Gd_{51}Al_{24}Co_{20}Zr_4Nb_1$ BMGs showing the glass transition and crystallization.

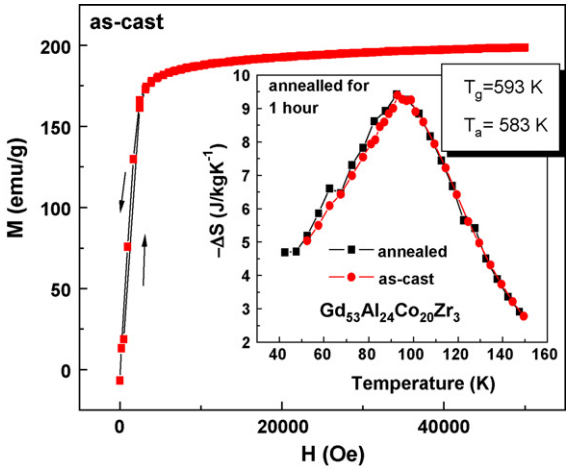

Fig. 4. Magnetic hysteresis of $Gd_{51}Al_{24}Co_{20}Zr_4Nb_1$ BMGs at 2 K. The inset shows the entropy changes of the as-cast and the annealed one just below T_g for 1 h for $Gd_{53}Al_{24}Co_{20}Zr_3$.

a relevant parameter characterizing the refrigerant efficiency of the material which can be calculated by different methods [44–46]. The RC is determined by numerically integrating the area under the ΔS_m–T curve, using temperatures at half-maximum of the peak as the integration limits. The RC values for $Gd_{53}Al_{24}Co_{20}Zr_3$ and $Gd_{51}Al_{24}Co_{20}Zr_4Nb_1$ determined by this method are 590 and 651 J kg^{-1}, respectively. These values are much larger than those of $Gd_5Si_2Ge_2$ (305 J kg^{-1}) and $Gd_5Si_2Ge_{1.9}Fe_{0.1}$ (360 J kg^{-1}) [3], indicating the better refrigerant efficiency of the Gd-based BMGs. The better RC is due to the glassy structure extends the large MCE to larger temperature range. For application, if a material exhibits large value of $-\Delta S_m$ at the transition temperature but falls off rapidly on either side, it is not suitable for use in Ericsson-cycle. In our case, we can obtain nearly the same values of magnetic entropy in wide temperature range for $Gd_xR_yAl_{24(25)}T_zM_{76-x-y-z}$ (where $x \sim 30$–60, R is Y, Zr or other rare earth element, T is Co or Ni, M is any transition element) alloys. Thus, the features of considerable $-\Delta S_m$ over a wide temperature range in the BMGs are favored in Ericsson-cycle.

The MCE of other heavy rare earth-based BMGs such as $Ho_{30}Y_{26}Al_{24}Co_{20}$ and $Dy_{50}Gd_7Al_{23}Co_{20}$ has also been studied. Unlike the ferromagnetic behavior of Gd-based BMGs, these alloys show typical spin glass-like frozen behavior [41], which is further exhibited by the temperature-dependent ac susceptibility of $Ho_{30}Y_{26}Al_{24}Co_{20}$ at different frequencies ranging from 10 to 10^4 Hz under an ac magnetic field of 10 Oe. The peak temperature $T_f(\omega)$ shifts towards higher temperature and the height of the susceptibility decreases with increasing frequency. The transition temperatures (T_f) for $Ho_{30}Y_{26}Al_{24}Co_{20}$ and $Dy_{50}Gd_7Al_{23}Co_{20}$ determined from the ZFC curves are 5.5 K and 26 K, respectively. Fig. 5(a) shows the $-\Delta S_m$ as a function of temperature under 2 T and 5 T for $Ho_{30}Y_{26}Al_{24}Co_{20}$, $Dy_{50}Gd_7Al_{23}Co_{20}$ and $Er_{50}Al_{24}Co_{20}Y_6$ BMGs [41]. Fig. 5(b) shows the $-\Delta S_m$ as a function of temperature under 5 T for typical heavy rare earth-based BMGs. From Fig. 5(a) the peak values of $-\Delta S_m$ under 5 T are 10.76 J kg^{-1} K^{-1} at temperatures of maximum, $T_p \sim 12$ K, 9.77 J kg^{-1} K^{-1} at $T_p \sim 45.5$ K and 15.91 J kg^{-1} K^{-1} at $T_p \sim 9.5$ K for $Ho_{30}Y_{26}Al_{24}Co_{20}$, $Dy_{50}Gd_7Al_{23}Co_{20}$ and $Er_{50}Al_{24}Co_{20}Y_6$, respectively. For $Tb_{36}Al_{24}Co_{20}Y_{20}$, due to a few crystalline phases embedded in the amorphous phase, its magnetic entropy change is smaller [41]. The peak values of $-\Delta S_m$ for Dy-, Ho- and Er-based BMGs are comparable with or even larger than those of Gd-based BMGs. Under 2 T, the peak slightly move to lower temperature compared with that of 5 T, and the peak values of $-\Delta S_m$ are determined to be 5.43 (J kg^{-1} K^{-1}), 4.33 (J kg^{-1} K^{-1}) and 8.57 (J kg^{-1} K^{-1}) for $Ho_{30}Y_{26}Al_{24}Co_{20}$, $Dy_{50}Gd_7Al_{23}Co_{20}$ and $Er_{50}Al_{24}Co_{20}Y_6$, respectively. Compared with that of the materials used in the similar temperature range, these values are comparable with or even higher than that of previously published results [47] for compounds with the same field variation (2 T): e.g. ~5 J kg^{-1} K^{-1} for $ErAl_2$, ~2 J kg^{-1} K^{-1} for $DyAl_2$, ~3 J kg^{-1} K^{-1} for $DyNi_2$, and larger than those of the families of $Dy_{1-x}Er_xAl_2$ and $Tb_xY_{1-x}Al_2$ [47–49], which show entropy changes of 2–5 J kg^{-1} K^{-1} and 1.2–7.6 J kg^{-1} K^{-1}, respectively. The RC values for $Ho_{30}Y_{26}Al_{24}Co_{20}$, $Dy_{50}Gd_7Al_{23}Co_{20}$ and $Er_{50}Al_{24}Co_{20}Y_6$ are 241, 290 and 423 J kg^{-1}, respectively. These values are smaller than those of Gd-based BMGs, but are comparable with those of the Gd–Si–Ge, Mn–Fe–Ge, Mn–Fe–P–As series, and larger than Ni–Mn–Ga series and most of the Fe- and Co-based glass ribbons. Comparing of the reported properties, magnetocaloric properties of different materials usually face the problems with the different experimental capabilities from one laboratory to another, and the different methods are usually adopted by different authors. For clarity of comparison we listed some typical materials including ours in Table 1 with the peak value of $-\Delta S_m$ and the RC which are calculated by the same method.

Compared with Gd-based BMGs, these random anisotropy magnets exhibit some interesting features. One is that the T_p of $-\Delta S_m$ are much larger than their T_f determined from low field magne-

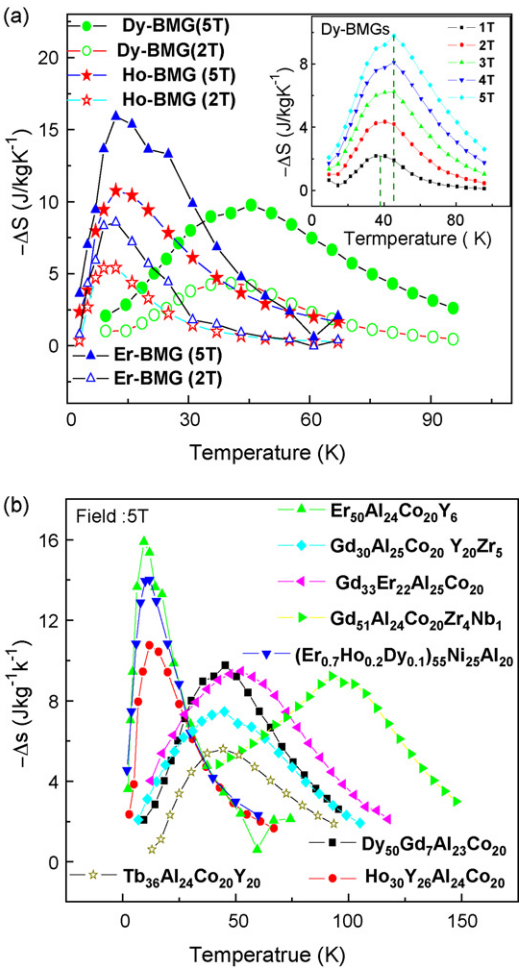

Fig. 5. (a) Magnetic entropy changes as a function of temperature for the as-cast $Ho_{30}Y_{26}Al_{24}Co_{20}$, $Dy_{50}Gd_7Al_{23}Co_{20}$ and $Er_{50}Al_{24}Co_{20}Y_6$ under 2 T and 5 T. The inset shows the magnetic entropy changes under different of fields for $Dy_{50}Gd_7Al_{23}Co_{20}$ [41]. (b) Magnetic entropy changes under 5 T for typical Gd-, Tb-, Dy-, Ho- and Er-based BMGs for comparison.

tization, especially for $Ho_{30}Y_{26}Al_{24}Co_{20}$ ($T_p \sim 12$ K, $T_f \sim 5.5$ K) and $Dy_{50}Gd_7Al_{23}Co_{20}$ ($T_p \sim 45.5$ K, $T_f \sim 26$ K). This may be due to the fact that high field strengthens ferromagnetic coupling of spins (spin clusters) from the beginning temperature (larger than T_f). For the magnetic entropy changes of $Dy_{50}Gd_7Al_{23}Co_{20}$ under different fields that the T_p reduced obviously as the maximum field reduces from 5 to 1 T [41]. The second is that the $-\Delta S_m$ is severe asymmetrical at two sides of their peak values. Long tails extend to much higher temperature than the T_p, but below the T_p, the value of $-\Delta S_m$ drops down much rapidly. This may result from the strong random magnetic anisotropy and exchange interaction frustration associated with spin glass frozen behavior due to disorder structure below T_p. Because it hinters the spin rotating with the applied external field and then the $-\Delta S_m$ becomes much smaller. The magnetic anisotropy effect can also be exhibited in the magnetic hysteresis behavior. Magnetic hysteresis was evaluated by the comparison of increasing and decreasing field magnetization process. At 2 K all these Ho-, Dy-, Tb-, Er-based BMGs show obvious hysteresis (not shown here), indicating that these alloys are magnetic harder than Gd-based BMGs. However, for the Ho- and Er-based BMGs, little hysteresis exists above 4 K. In $Dy_{50}Gd_7Al_{23}Co_{20}$ moderate hysteresis is still observed at 9 K, when temperature increases to 16 K the hysteresis becomes much smaller. Near and above T_f, no magnetic hysteresis is observed in the paramagnetic (superparamagnetic) region. Thus, all the alloys are magnetic soft near and above spin freezing temperature.

3.3. The effects of structural change induced by aging and crystallization on MCE

Due to its intrinsic unstable or metastable nature, a glass usually continually relaxes to a more stable state accompanied with atoms rearrangement. Aging behavior in glass is important because it gives abundant information about the microstructure and the nature of the glassy state [50–52]. From the point of view of application, physical aging thus must be taken into account because it brings about changes in almost all physical properties. For the BMGs, the crystallization behavior poses special interesting scientific and practical questions [18–22]. Upon crystallization nanocrystallization occurs in many of these glasses, and their mechanical and many other properties can be then enhanced [53,54]. In fact, previous work showed that ferromagnetic materials containing nanometer-sized magnetic region and the nanometer superparamagnet have superior MCE over certain temperature and field intervals compared with the conventional bulk ferromagnetic and paramagnetic materials [55–58,49], and crystallization effects have also been studied in some Fe-based ribbon [10,59].

To understand the relationship between the MCE and the disorder structure, the influences of aging and crystallization behavior on the MCE of $Gd_{51}Al_{24}Co_{20}Zr_4Nb_1$ BMGs under a modest magnetic field have been investigated. The structural changes are detected by XRD and magnetization experiments. We use different capitals to represent samples isothermally annealed for different conditions in the vacuum chamber. The sample *A* was annealed at 673 K (T_g = 598 K) for 30 h, sample *B* was annealed at 613 K for 1 h, sample *C* was annealed at 703 K for 1 h, the sample *D* was annealed at 923 K for 5 h. From the XRD patterns in Fig. 6, one can clearly see that their structure is changed after annealing. The amorphous structure was maintained in sample *A* and thus only structure relaxation happened. For sample *B* few nanocrystalline particles can be detected from the XRD pattern. After annealed at 703 K (between T_{x1} and T_{x2}) for 1 h, larger amount of crystalline particles are formed. For sample *D* no amorphous phase can be detected and the BMG fully crystallized into multi-crystalline phases. The temperature dependence of the magnetization determined under 200 Oe for the as-cast $Gd_{53}Al_{24}Co_{20}Zr_3$ and the annealed ones shows the aging

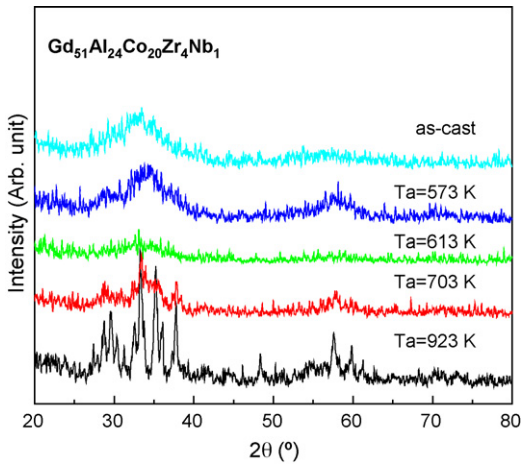

Fig. 6. XRD patterns taken from the cross-sectional slices of the as-quenched and annealed ones for $Gd_{51}Al_{24}Co_{20}Zr_4Nb_1$.

and crystallization change the magnetic properties obviously and lead to reduction of the T_c, but after full crystallization the T_c slightly increased due to some special crystalline phase. Furthermore, in contrast to the sharp transition near T_c of the as-cast sample, the transition is smeared out obviously for all the treated samples. At the same time the magnetization values below T_c go down obviously for the annealed samples. Thus reduction of the magnetic entropy change near the transition temperature can be anticipated.

Fig. 7 shows a series of isothermal magnetization curves for sample *D* from 24 to 150 K. These curves are different from those of as-cast sample and exhibit multi-phase character, especially in low temperature region. After aging below T_g the peak values of $-\Delta S_m$ reduces and the cusp also moves to lower temperature. The reduction is attributed to the atom and stress relaxation companied with short-range order structural change. We also studied the relaxation induced by short time annealing just below T_g in $Gd_{53}Al_{24}Co_{20}Zr_3$. As shown in the inset of Fig. 4, the traces are almost the same as that of the as-cast sample. This indicates that long time is needed to detect magnetic structural change even close to T_g. Due to their high T_g (far above room temperature), near room temperature and below, one can expect that no obvious structure relaxation occurs and thus the magnetic properties can keep stable. For slightly crystallized sample *B* and partially crystallized sample *C*, the peaks of $-\Delta S_m$ move to lower temperature, but the cusp of $-\Delta S_m$ moves to slightly higher temperature for fully crystallized sample *D*. These

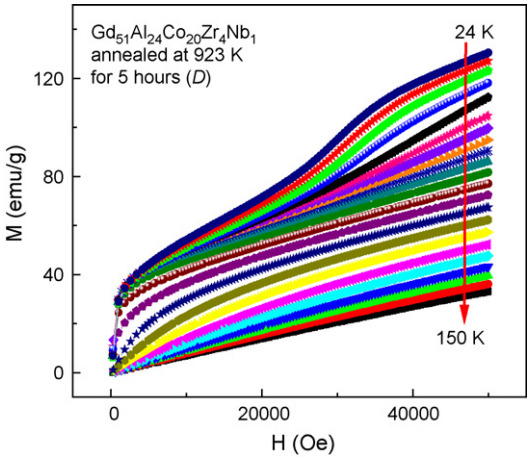

Fig. 7. Isothermal magnetization of full crystallized $Gd_{51}Al_{24}Co_{20}Zr_4Nb_1$ (sample *D*) as a function of magnetic field at various temperatures.

behaviors are consistent with the magnetization data. The crystallization, partially or fully, always result in a remarkable reduction of the peak values of the $-\Delta S_m$. Nevertheless, the reduced values are still much larger than those of the Fe- and Co-based glass ribbons [10–15].

Our study shows that structural disorder reduces the transition temperature and leads to a broader peak in the magnetic entropy change due to fluctuation of the exchange integral, but the refrigerant efficiency remains. However, for samples *C* and *D*, their multi-phase structure result in smearing out the transition, so the peak value of $-\Delta S_m$ decreases but makes the peaks broader. The superior MCE feature is thus obtained in the amorphous alloy in terms of the maximum of $-\Delta S_m$. The significant results in sample *D* is that the temperature variation of the MCE shows additional minimum below the transition temperature, and a table-like shape of the MCE, where a nearly constant magnetic entropy change over 21–50 K, has been obtained. A similar table-like MCE property has also been observed over a wide temperature range of 47–107 K in sample *C*. For practical application, the lattice entropy effect has to be removed in the range of $T > 20$ K, where Ericsson-cycle is usually utilized. The ideal magnetic refrigerants suitable for use in an Ericsson-type refrigerator should have a constant (or almost constant) through the thermodynamical cycle range. Thus, the materials, which have large MCE effect over a large temperature range for optimum efficiency, are of great interest and urgency to be utilized in an Ericsson-cycle. Usually, multi-layered structure materials are designed to meet this requirement [60–63], where ferromagnetic materials with varying Curie temperature are layered or sintered. Our results indicated that partially devitrification of the BMGs with nanocrystalline grains embedded in the amorphous matrix exhibit almost constant and relatively high magnetic entropy change over a large temperature range. Compared with the layered or sintered composites, the crystallization method owns its the advantage of convenience and makes the construction of active magnetic regenerator much simple. The partially crystallized BMGs could be promising working substances for Ericsson-cycle-type based magnetic refrigerator.

3.4. Alloying effects on MCE

For crystalline materials, even minor alloying additions can change the crystal structure and thus the magnetic properties of an alloy and reduces the MCE owing to the disappearance of first order phase transition [3,64–70]. For rapid quenched BMGs, this situation becomes interesting and subtle. The minor addition has significant impact on the formation, structure, crystallization, thermal stability and mechanical property of BMGs [22]. In order to enrich the understanding of the performance of MCE in these new kinds of materials, the effect of alloying additions of B, Cr, Ce, Y and Er on the structure and MCE was investigated.

Amorphous alloys with nominal compositions $Gd_{33}Er_{22}Al_{25}Co_{20}$, $Gd_{30}Al_{25}Co_{20}Y_{20}Zr_5$, $Gd_{51}Al_{24}Co_{20}B_4Nb_1$, $Gd_{51}Al_{24}Co_{20}Cr_4Nb_1$, $Gd_{51}Al_{24}Co_{20}Ce_5$ and $Gd_{48}Al_{25}Co_{20}Zr_3Er_4$ were prepared by the minor alloying in the form of cylindrical rods 2 or 3 mm in diameter [22]. Full amorphous structure was obtained in all of the alloys except $Gd_{51}Al_{24}Co_{20}B_4Nb_1$. In alloy $Gd_{51}Al_{24}Co_{20}B_4Nb_1$, crystalline phases with small fraction embedded in amorphous matrix. Fig. 8 shows the temperature dependence of magnetization for theses alloys, from which it is obviously that alloying addition of both magnetic Ce and Er, and nonmagnetic B can reduce the Curie temperature. It is noticed that reentrant spin glass-like behavior is observed for the 4% Er additional alloy, which may indicate that the antiferromagnetic coupling of Gd and Er moments. Substituting more amounts of Er and Y lead to spin glass-like frozen behavior at lower transition temperature for $Gd_{33}Er_{22}Al_{25}Co_{20}$ and $Gd_{30}Al_{25}Co_{20}Y_{20}Zr_5$. For

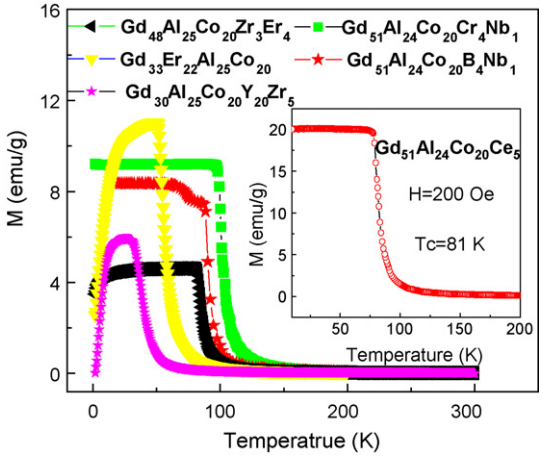

Fig. 8. The temperature dependence of the magnetization under100 Oe for $Gd_{48}Al_{25}Co_{20}Zr_3Er_4$ and $Gd_{30}Al_{25}Co_{20}Y_{20}Zr_5$, 200 Oe for other four.

$Gd_{51}Al_{24}Co_{20}Cr_4Nb_1$, the Curie temperature increases slightly which shows that proper addition of Cr can strengthen the exchange interaction of Gd. The reduction of T_c by replacing some percents of Gd with Er or Ce can be attributed to the lower magnetic interaction and lower transition temperature of Er and Ce. The determined magnetic entropy changes show that the alloying effects of Ce, Er and Cr can only tune the position of the peak of the $-\Delta S_m$ without changing the peak value and the refrigerant capacity of the alloy [41]. The slightly reduction of the peak value of $-\Delta S_m$ for B additional alloy are due to few crystalline phase in the amorphous matrix, similar to the partially crystallization effect. Substitution of as much as 20% Y brings slightly deleterious influence for magnetocaloric response but can tune the working temperature to much lower temperature. The alloying brings only slightly change of RC in all samples.

Besides the attractive refrigerant efficiency of the BMGs, the tunable feature of the working temperature by alloying over a large temperature range is also beneficial for practical application. Furthermore, $Gd_xR_yAl_{24(25)}T_zM_{76-x-y-z}$ series (R is Y, Zr or other rare earth element, T is Co or Ni, M is any transition element) with varying transition temperature can also be mixed or layered to get nearly constant $-\Delta S_m$ over a broad temperature range for application in Ericsson-cycle. On the other hand, our study shows that although microalloying can have some influence on the atomic structure, but it does not bring considerable impact on the MCE as it can do on the glass-forming ability and the mechanical properties [22].

3.5. Field dependence of the magnetocaloric effects

For the minor alloying and aging effects which can tune the microstructure, the working temperature can be extended and the performance may be enhanced. Furthermore, according to the Maxwell relation, the magnetic entropy change depends on the value of the maximum applied field. And understanding this dependence can give much information about the physics of the magnetocaloric effect near the transition temperature. For materials with a second order phase transition (just as these BMGs), a mean field picture predicted [71]: $\left|\Delta S_m^{pk}\right| \propto H^n$ where $\left|\Delta S_m^{pk}\right|$ is the peak magnetic entropy change and $n = 2/3$. However, experimental results [72] of some soft Fe-based glassy ribbons deviate from the value of n near the transition temperature. For get a deeper insight into the nature of the MCE of BMGs, we investigated the field dependence of MCE for two typical samples $Gd_{51}Al_{24}Co_{20}Zr_4Nb_1$ and $Dy_{50}Gd_7Al_{23}Co_{20}$ in temperature range

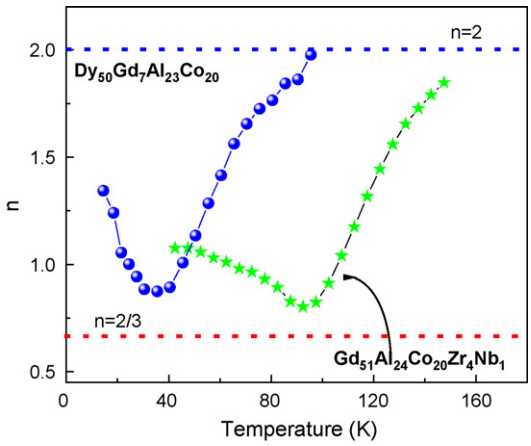

Fig. 9. Temperature dependence of the local exponent n for two BMGs. The lines are a guide to the eyes.

from well below to well above the transition temperature. The two BMGs are specially picked out because the Gd-based BMG is very soft in the whole temperature range and frozen into ferromagnetic state below the transition temperature, while the Dy-based BMG frozen into spin glass-like state and is magnetic harder below its transition temperature due to its strong random magnetic anisotropy.

We analyzed the field dependence of $-\Delta S_m$ using the relation $|\Delta S_m| \propto H^n$ suggested for a mean field case. As shown in Fig. 9, far above the transition temperature where Curie–Weiss law is well satisfied, n is approaching to 2. This behavior can well be understood, because in this high temperature limit range the magnetization has a linear field dependence, and the Maxwell relation results in a quadratic field dependence of $-\Delta S_m$. The largest values of n obtained in this temperature range reflect the most sensitivity of magnetic entropy to external filed change. With decreasing temperature (above the transition temperature) n is decreasing gradually as the Curie–Weiss law deviates and the shot range magnetic order forms gradually. From the two curves in Fig. 9, it can be seen that the field dependence of magnetic entropy are very similar above the transition temperature and also similar to other glassy alloys.

The interesting behaviors are around and below the transition temperature. The lowest value of n near the transition temperature, is ~0.81 for Gd-based BMG and ~0.87 for Dy-based BMG, both of which are larger than 2/3 as predicted by the mean field model and are also larger than those of Fe-based glassy ribbons ($n \sim 0.73$). This deviation of the mean field value near transition temperature is not surprising because of its usual failure for the description of materials near transition temperature. With decreasing temperature further below the transition temperature, n increases gradually. For some glassy alloys [69] n is approaching to 1 gradually in the low temperature limit. This behavior can be simply understood if the magnetization show little field dependence or the magnetization can be written as $M(H, T) = Ms(T) + F(H)$, where the $Ms(T)$ is the spontaneous magnetization and $F(H)$ is temperature independent. This is likely the case for Gd-based BMG of which the n approaches a value slightly larger than 1. However, this simple assumption is not applicable to the Dy-based BMGs in the temperature and field range investigated, since the values of n in the low temperature states can be as large as 1.34. Its values between 1 and 2 suggest the magnetization depends on the temperature but weaker than a linear temperature dependence case. The significant difference between the two alloys indicates that the values of n for Dy-BMG can be larger and increase faster with decreasing temperature than those of Gd-BMG.

4. Conclusions

The high performances of magnetic refrigerants have been obtained in heavy rare earth-based BMGs over wide range of transition temperatures between 2 and 100 K. Structural disorder reduces the transition temperature not the large magnetic entropy change of the BMGs. On the contrary, it broadens the value of $-\Delta S_m$ and results in the increased RC. The unique structure in glassy alloys, in which the distance between adjacent atoms, the coordination number, and the chemical environment varies from site to site, results in a distribution of exchange interaction. So, the broad peak of magnetic entropy change is a disorder structure induced intrinsic property of the BMGs. Furthermore, the MCE of BMG can be modulated by aging and crystallization. The aging and partially crystallization lead to the reduction of transition temperature and the peak value of $-\Delta S_m$, while table-like shapes of the MCE covering wide temperature range is formed for the crystallized sample. Compared with the multi-layered structure, the glassy alloys and corresponding crystallized composites take the advantage of the low cost and much facility in manufacture without the problem of solid-state reactions between constituent materials which is usually encountered in multi-layered materials. The devitrification of the BMGs is a promising route to prepare nanocrystalline materials presenting interesting properties for magnetic refrigeration. Another advantage of these BMGs is their facile tunable character by alloying or substituting, which makes the working temperature of these kinds of materials cover a wide temperature range. The composites can be synthesized by using series of rare earth-based BMGs with different ordering temperature to obtain nearly constant magnetic entropy change for usage in the Ericsson-cycle. Combined with their good glass-forming ability, high thermal stability, considerable facility for thermal treatment and relatively free of hysteresis near and above the transition temperature, these metallic glassy materials can serve as promising candidates for magnetic refrigerants and for fundamental study.

The field dependence of the magnetic entropy change shows power dependence in temperature and field range investigated for typical Gd-based BMG and Dy-based BMG with a second order phase transition. Both alloys share similar behavior above the transition temperature, especially in the high temperature limit, and the local exponent n is ~2 as a result of the Curie–Weiss law. Just near the transition temperature both alloys deviate the mean field value indicating the insufficient description of the mean filed picture at the transition temperature, and n is slightly larger for Dy-based BMG than that of Gd-based BMG. However, in the low temperature limit obvious differences occur due to their different magnetic structure of the two alloys. The strong random magnetic anisotropy in the $Dy_{50}Gd_7Al_{23}Co_{20}$ not only leads to spin glass-like state different from the ferromagnetic state of Gd-based BMG, but also has clearly influence on the field dependence of the magnetic entropy change. The anisotropy interaction makes the $-\Delta S_m$ more sensitive to the fields in the low temperature range reflecting in its larger n compared with that of Gd-based BMG.

Acknowledgements

Financial support from the National Natural Science Foundation of China (Grant Nr. 50921091) and the National Basic Research Program of China (MOST 973, Grant Nr. 2007CB613904) are gratefully acknowledged. The experimental assistance and discussions of D.Q. Zhao, M.X. Pan are appreciated.

References

[1] N.A. de Oliveira, J. Alloys Compd. 455 (2008) 81–86.
[2] Z.B. Guo, Y.W. Du, H. Huang, D. Feng, Phys. Rev. Lett. 78 (1997) 1142.

[3] V. Provenzano, A.J. Shapiro, R.D. Shull, Nature 429 (2004) 853.
[4] K. Fukamichi, A. Fujita, S. Fujieda, J. Alloys Compd. 408–412 (2006) 307–312.
[5] A.M. Tishin, J. Alloys Compd. 250 (1997) 635–641.
[6] E. Talik, M. Klimczak, J. Alloys Compd. 486 (2009) L30–L33.
[7] X.X. Zhang, G.H. Wen, F.W. Wang, Appl. Phys. Lett. 77 (2000) 3072.
[8] V. Recarte, J.I. Pérez-Landazabál, C. Gómez-Polo, E. Cesari, J. Dutkiewicz, Appl. Phys. Lett. 88 (2006) 132503.
[9] T.D. Shen, R.B. Schwarz, J.Y. Coulter, J.D. Thompson, J. Appl. Phys. 91 (2002) 5240.
[10] P. Didukh, A. Slawska-Waniewska, J. Magn. Magn. Mater. 254–255 (2003) 407.
[11] S. Atalay, H. Gencer, V.S. Kolat, J. Non-Cryst. Solids 351 (2005) 2373.
[12] S.G. Min, K.S. Kim, H.S. Suh, S.W. Lee, J. Appl. Phys. 97 (2005) 10M310.
[13] V. Franco, J.S. Blázquez, A. Conde, Appl. Phys. Lett. 88 (2006) 042505.
[14] K. Burian, M. Kowalczyk, R. Kolano, R. Szymczak, H. Szymczak, M. Polak, J. Alloys Compd. 479 (2009) 71–73.
[15] K.S. Kim, S.G. Min, S.C. Yu, S.K. Oh, Y.C. Kim, K.Y. Kim, J. Magn. Magn. Mater. 304 (2006) 642.
[16] Q. Luo, D.Q. Zhao, M.X. Pan, R.J. Wang, W.H. Wang, Appl. Phys. Lett. 89 (2006) 081914.
[17] M. Foldeaki, R. Chahine, B.R. Gopal, T.K. Bose, X.Y. Liu, J.A. Barclay, J. Appl. Phys. 83 (1998) 2727.
[18] W.L. Johnson, MRS Bull. 24 (1999) 42.
[19] A. Inoue, T. Zhang, Mater. Trans. 30 (1989) 965.
[20] W.H. Wang, J. Non-Cryst. Solids 351 (2005) 1481–1485.
[21] W.H. Wang, C. Dong, C.H. Shek, Mater. Sci. Eng. R 44 (2004) 45.
[22] W.H. Wang, Prog. Mater. Sci. 52 (2007) 540.
[23] X.K. Xi, L.L. Li, B. Zhang, W.H. Wang, Y. Wu, Phys. Rev. Lett. 99 (2007) 095501.
[24] S. Li, M.X. Pan, D.Q. Zhao, W.H. Wang, Sci. Tech. Adv. Mater. 6 (2005) 823.
[25] S. Li, M.X. Pan, D.Q. Zhao, W.H. Wang, J. Non-Cryst. Solids 351 (2005) 2068.
[26] S. Li, D.Q. Zhao, W.H. Wang, Scripta Mater. 53 (2005) 1489.
[27] S. Li, D.Q. Zhao, W.H. Wang, J. Non-Cryst. Solids 354 (2008) 1080.
[28] Z.F. Zhao, Z. Zhang, D.Q. Zhao, W.H. Wang, Appl. Phys. Lett. 82 (2003) 4699.
[29] Z. Zhang, L. Xia, M.X. Pan, W.H. Wang, Appl. Phys. Lett. 81 (2003) 4371.
[30] B.C. Wei, W. Löser, W.H. Wang, J. Eckert, Acta Mater. 50 (2003) 4357.
[31] B.C. Wei, Y. Zhang, D.Q. Zhao, W.H. Wang, J. Appl. Phys. 89 (2001) 3529.
[32] X.K. Xi, S. Li, D.Q. Zhao, M.X. Pan, W.H. Wang, J. Mater. Res. 20 (2005) 2243.
[33] B.C. Wei, W.H. Wang, M.X. Pan, W.R. Hu, Phys. Rev. B 64 (2001) 012406.
[34] Q. Luo, D.Q. Zhao, M.X. Pan, W.H. Wang, Appl. Phys. Lett. 88 (2006) 181909.
[35] Y.X. Wei, B. Zhang, D.Q. Zhao, M.X. Pan, W.H. Wang, Scripta Mater. 54 (2006) 599.
[36] B. Zhang, M.X. Pan, D.Q. Zhao, W.H. Wang, Phys. Rev. B 70 (2004) 224208.
[37] B. Zhang, M.X. Pan, D.Q. Zhao, W.H. Wang, Appl. Phys. Lett. 85 (2004) 61.
[38] B. Zhang, D.Q. Zhao, M.X. Pan, W.H. Wang, A.L. Greer, Phys. Rev. Lett. 94 (2005) 205502.
[39] B. Zhang, D.Q. Zhao, M.X. Pan, W.H. Wang, Acta Mater. 54 (2006) 3025.
[40] W.H. Wang, J. Appl. Phys. 99 (2006) 093506.
[41] Q. Luo, W.H. Wang, J. Non-Cryst. Solids 355 (2009) 759–775.
[42] W.H. Wang, Adv. Mater. 21 (2009) 4524–4544.
[43] S. Stadler, M. Khan, J. Mitchell, N. Ali, A.M. Gomes, I. Dubenko, A.Y. Takeuchi, A.P. Guimarães, Appl. Phys. Lett. 88 (2006) 192511.
[44] Q. Luo, D.Q. Zhao, M.X. Pan, W.H. Wang, Appl. Phys. Lett. 90 (2007) 211903.
[45] M.E. Wood, W.H. Potter, Cryogenics 25 (1985) 667.
[46] K.A. Gschneidner, V.K. Pecharsky, Mater. Sci. Forum 315–317 (1999) 69.
[47] X. Bohigas, J. Tejada, F. Torres, J.I. Arnaudas, E. Joven, A. del Moral, Appl. Phys. Lett. 81 (2002) 2427.
[48] P.J. von Ranke, V.K. Pecharsky, K.A. Gschneidner, Phys. Rev. B 58 (1998) 12110.
[49] Q. Zhang, J. Du, Y.B. Li, N.K. Sun, W.B. Cui, D. Li, Z.D. Zhang, J. Appl. Phys. 101 (2007) 123911.
[50] I.M. Hodge, Science 267 (1995) 1945.
[51] C.A. Angell, Science 267 (1995) 1924.
[52] Q. Luo, D.Q. Zhao, M.X. Pan, R.J. Wang, W.H. Wang, Appl. Phys. Lett. 88 (2006) 151915.
[53] B.S. Murty, K. Hono, Mater. Sci. Eng. A 312 (2001) 253.
[54] A. Revesz, P. Ochin, P. Donnadieu, J.P. Simon, P. Guyot, Phil. Mag. Lett. 81 (2001) 767.
[55] R.D. McMichael, J.J. Ritter, R.D. Shull, J. Appl. Phys. 73 (1993) 6946.
[56] R.D. McMichael, R.D. Shull, L.H. Bennett, C.D. Fuerst, J.F. Herbst, NanoStructured Mater. 2 (1993) 277.
[57] R.D. Shull, IEEE Trans. Magn. Mag. 29 (1993) 2614.
[58] D.Y. Chen, S. Patel, D.T. Shaw, J. Magn. Magn. Mater. 134 (1994) 75.
[59] D. Wang, K. Peng, B. Gu, Z. Han, S. Tang, W. Qin, Y. Du, J. Alloys Compd. 358 (2003) 312.
[60] T. Hashimoto, T. Kuzuhara, M. Sahashi, K. Inomata, A. Tomokiyo, H. Yayama, J. Appl. Phys. 62 (1987) 3873.
[61] Z. Yan, J. Chen, J. Appl. Phys. 72 (1992) 1.
[62] G.S. Burkhanov, S.Yu. Dan'kov, S.A. Nikitin, A.M. Tishin, O.D. Chistyakov, Sov. Tech. Phys. Lett. 17 (1991) 353.
[63] A. Smaïli, R. Chahine, J. Appl. Phys. 81 (1997) 824.
[64] V.K. Pecharsky, K.A. Gschneidner, J. Magn. Magn. Mater. 167 (1999) L179.
[65] Z. Han, Z. Hua, D. Wang, C. Zhang, B. Gu, Y. Du, J. Magn. Magn. Mater. 302 (2006) 109.
[66] W.H. Wang, Q. Wei, H.Y. Bai, Appl. Phys. Lett. 71 (1997) 58–60.
[67] W.H. Wang, Q. Wei, H. Wollenberger, Appl. Phys. Lett. 71 (1997) 1053–1055.
[68] Z. Bian, M.X. Pan, Y. Zhang, W.H. Wang, Appl. Phys. Lett. 81 (2002) 4739–4741.
[69] Y.X. Zhuang, W.H. Wang, Y. Zhang, M.X. Pan, D.Q. Zhao, Appl. Phys. Lett. 75 (1999) 2392–2394.
[70] W.H. Wang, Z. Bian, P. Wen, Y. Zhang, M.X. Pan, D.Q. Zhao, Intermetallics 10 (2002) 1249–1257.
[71] H. Oesterreicher, F.T. Parker, J. Appl. Phys. 55 (1984) 4334.
[72] V. Franco, J.M. Borrego, C.F. Conde, M. Stoica, S. Roth, J. Appl. Phys. 100 (2006) 083903.